ION-ACOUSTIC WAVE ACTIVITY IN $m = 0$ HELICON PLASMAS

K.P. Shamrai, V.F. Virko, V.M. Slobodyan, Yu.V. Virko, G.S. Kirichenko
Institute for Nuclear Research, National Academy of Sciences
47 Prospect Nauki, 03680 Kiev, Ukraine

The results of experimental and theoretical study of low-frequency (LF) wave activity in a helicon plasma and in an inductively coupled magnetized plasma are presented. This activity is shown to relate to ion-acoustic (IA) waves whose spectra can be either noise and continuous, or spiky, or combined. The origin of activity is ascertained from correlative measurements of wave characteristics, stationary plasma parameters, and plasma diamagnetic response. Various driving mechanisms of the IA waves are discussed.

PACS: 52.35.Fp

1. INTRODUCTION

Ion-acoustic (IA) turbulence in helicon plasmas was originally predicted theoretically to result from kinetic parametric instability and to contribute substantially to plasma heating [1,2]. IA turbulence was measured in various experiments on different devices using both microwave [3,7] and probe [4-7] diagnostics. Spectra of turbulence were found to be either continuous and broadband [3,5,7], or spiky [6], or to include both continuous and spiky components [4,6]. Besides kinetic parametric instability [1,2], hydrodynamic parametric instabilities, such as decay [4,7] and oscillating two-stream ones [5] were also examined as drivers of the IA waves. The role of the nonlinear parametric mechanism was argued experimentally: it was shown that the IA waves and the HF waves in sidebands of the pumping frequency satisfy matching conditions on frequencies and wave numbers [4,7], and that the IA waves have excitation threshold on the rf power [5,7]. The linear mechanism, viz, the electron drift current driven instability was also considered as a pretender to excitation of the IA waves [6].

We report on probe measurements of the low-frequency (LF) waves in two different devices, the helicon plasma and the inductively coupled magnetized plasma, both driven by $m = 0$ antennas, and on theoretical analyses of mechanisms capable of driving the LF wave activity. In Sec.2, measurements of both the LF waves and high-frequency (HF) waves in sidebands around the driving frequency performed in the helicon plasma are described along with measurements of the diamagnetic signal and stationary plasma parameters. Section 3 deals with the spectra and spatial distributions of the LF oscillations measured correlatively with profiles of static plasma parameters in the inductively coupled magnetized plasma. Theoretical analyses of driving mechanisms of the IA activity; i.e., the kinetic electron drift current driven instability, the hydrodynamic parametric instability excited in a combined field of the helicon wave and quasi-electrostatic wave arising due to linear mode conversion, and the instability excited under combined action of both non-equilibrium factors is presented in Sec.4. Section 5 gives conclusions.

2. WAVES IN THE HELICON PLASMA

Experiments were performed in the helicon source described elsewhere [5,8]. It consists of a 14-cm-diameter, 23-cm-long quartz tube attached to a 14-cm-long metal section of the same diameter and is limited by a metal flange, at z=0, and by a copper grid, at z=36 см. The magnetic field produced by two identical coils could be either uniform, with both coils equally powered, or nonuniform, with one of the coils turned off. The discharge was excited by a double-turn (m=0) antenna positioned at z=6 cm and supplied from a 13.56 MHz, 1 kW rf generator. The following standard conditions were normally applied: absorbed power 1 kW and Ar pressure 5 mTorr. The average density was measured by an 8-mm interferometer, while plasma and wave characteristics by the Langmuir probes, by the multi-purpose single-loop probe that could operate as the electric, magnetic, or emissive probe, and by the rotatable binary probe. The discharge was normally operated continuously, but it could be terminated abruptly to measure the diamagnetic signal by a 100-turn belt overlapping the quartz chamber at z =18 cm.

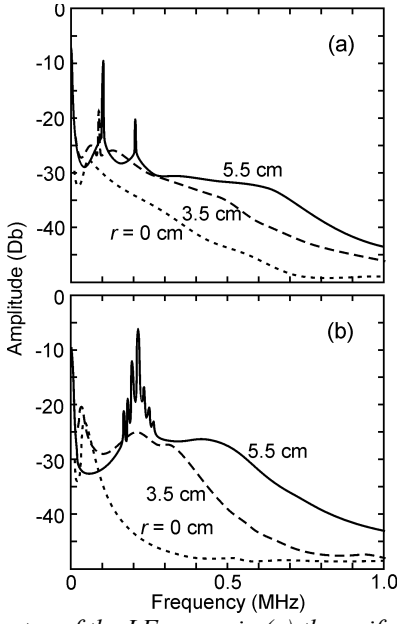

Fig.1. Spectra of the LF waves in (a) the uniform and (b) the nonuniform magnetic field

If the magnetic field is uniform, LF oscillations have continuous, noise spectrum whose intensity and width grow to the periphery (Fig.1,a). Closer to the periphery, there arise one or two intense spikes in the range 0.1… 0.2 MHz. In the nonuniform field, the spectrum has a continuous, noise component; closer to the periphery, it includes a set of spikes located around 0.2 MHz and separated by 12.5 kHz (Fig.1,b).

Noise oscillations in all cases were measured to be IA waves that propagate with the IA velocity, $v_S \approx 3\times 10^5$ cm·s^{-1}, and obliquely in cross-section (azimuthally – along electron gyration, and radially – towards the plasma periphery), at 45…60° to the radius. These waves produce density variations of the order of $\delta n/n \le 1\%$. Waves related to spikes exist only at the periphery, propagate azimuthally with the IA velocity and demonstrate excitation threshold on the rf power. These waves are the global IA eigenmodes, which have high azimuthal numbers m =10...17 and propagate in the opposite directions in the uniform and nonuniform magnetic field, just along electron drift streams detected with the diamagnetic loop.

Spectra of HF waves around the driving frequency also include continuous and spiky components and reproduce fairly the shape of LF spectra. These spectra in the nonuniform field are shown in Fig.2. Two intense sideband peaks (r = 4.4 cm) consist of a set of spikes spaced by 12.5 kHz, the same as spacing of the LF spikes at r=5 cm. The spectrum at r =3.5 cm is the same in shape as the LF spectrum at r = 3 cm.

Noise components of the sideband spectra in capacitive signal are mirror symmetric relative to 13.56 MHz. In addition, these oscillations demonstrate interference patterns that are similar to those for the LF noise oscillations. For this reason, they are not potential waves and arise, apparently, due to variation of plasma density by the IA waves which alters the sheath width and, thus, the probe–plasma capacitance.

Sideband spectra in the magnetic signal are found to be asymmetric, with lower sideband being stronger. Similarly to the LF spectra, sideband spectra include the discrete spikes related to waves which have azimuthal phase velocities $(2.5\ldots4.5)\times10^7$ cm·s^{-1} and propagate oppositely in the lower and upper sidebands, and in the uniform and nonuniform magnetic field.

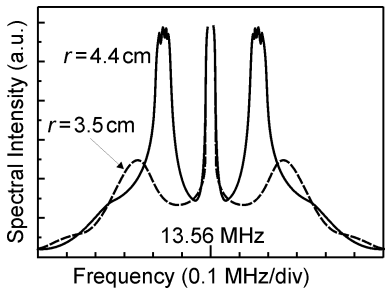

Fig.2. HF spectra in the nonuniform magnetic field

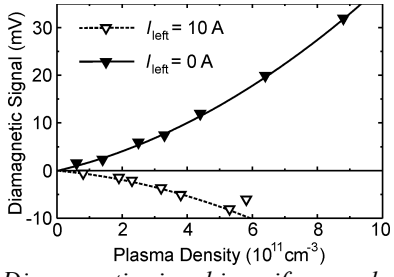

Fig.3. Diamagnetic signal in uniform and nonuniform fields

The lower spiky sideband HF wave (ω,k) and its IA partner (ω_S,k_S) have equal wavelengths but propagate oppositely, and the phase velocity of the HF wave fits well the relation $\omega/|k_S|$ where ω_0 is the pump frequency. As these waves satisfy the decay matching conditions on frequencies, $\omega = \omega_0 - \omega_S$, and wave numbers, $k = -k_S$, they are thought to arise from the parametric instability.

Obtained results apparently evidence that the IA waves from continuous spectra are excited by the azimuthal electron drift current, as was observed in other experiments (e.g., [9]). We detected these currents at the discharge break up, with use of the diamagnetic belt. Diamagnetic plasma response as function of the before-breaking plasma density is shown in Fig.3. It demonstrates diamagnetic (paramagnetic) polarity in the nonuniform (uniform) magnetic field. We also measured the diamagnetic signal at a fixed rf power but varying the left coil current. With increasing magnetic field nonuniformity, the signal was found to change the polarity while the plasma density to grow.

To determine the origin of the drift currents, we measured the distributions of static plasma parameters. Radial profiles of electron density and temperature measured at z =18 cm in the nonuniform field are shown in Fig.4. Electron pressure profile deduced from these data is also shown; it is flat except at the periphery. In this region, the velocity of diamagnetic electron current is estimated to exceed (5…10)-times the IA velocity. In the uniform magnetic field, the pressure gradient is found to be small right to the wall, so that diamagnetic current is negligible.

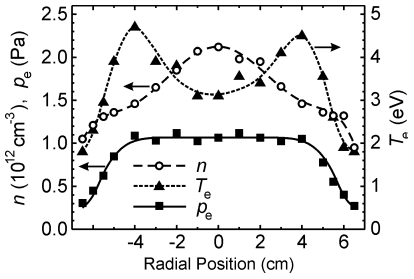

Fig.4. Electron density, temperature and pressure profiles in the nonuniform field, at z = 18 cm

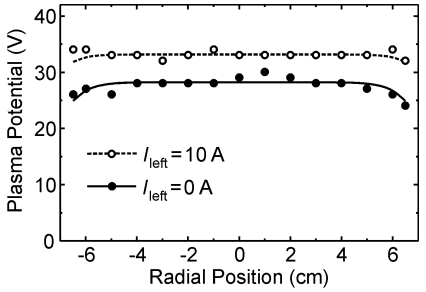

Fig.5. Radial profiles of the plasma potential, at z= 18 cm

Radial profiles of the plasma potential, which are shown in Fig.5 for z =18 cm, are quite flat in both the uniform and nonuniform fields and are found to have similar shapes along the whole discharge length. Note that the radial field of the order of 1 V·cm^{-1} would be

enough to produce the electric drift compatible with the diamagnetic drift; however, in our measurements we could not detect the field so accurately.

3. WAVES IN INDUCTIVELY COUPLED MAGNETIZED PLASMA

Another source used in our experiments and described elsewhere [10] consists of a 20-cm-diameter, 30-cm-long cylindrical metal chamber limited by a metal substrate table from below (z =30 cm) and by a quartz window from above (z = 0 cm). The discharge in Ar was excited by a 17.5-cm-diameter single-loop (m=0) flat antenna positioned above the window and powered from the rf generator of frequency 13.56 MHz and power up to 1.5 kW. Three magnetic coils with separate current control produced nonuniform magnetic field whose shape was mostly dependent on the upper coil current, I_{up}, and was found to have a significant effect on plasma parameters and wave processes. Experiments were performed at a fixed rf power of 750 W and Ar pressure of 3.8 mTorr and at varying I_{up}. We used the electric, thermo-emissive, and binary (correlation) probes for measurements.

Strong dependence of the discharge regimes on magnetic configuration is displayed as abrupt density jumps at continuous variation of I_{up} [10], which occur over the whole plasma cross-section. Plasma density profiles also alter considerably, as seen from Fig.6, and show strong gradients in some regimes.

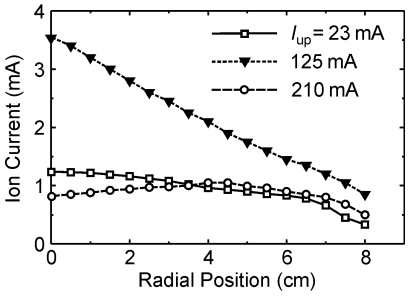

Fig.6. Radial profiles of ion saturation current, at z= 25 cm

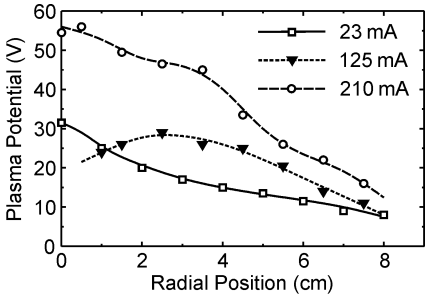

Fig.7. Radial profiles of the plasma potential, at various I_{up}

Radial profiles of the plasma potential measured with the thermo-emissive probe are shown in Fig.7. As seen, in some regimes quite strong radial electric fields (up to 5 V·cm^{-1}) arise in plasma. Note that the difference between the floating and plasma potentials could be as large as 70 V, which evidences presence of non-equilibrium electrons.

LF wave activity is inherent to plasma in all the discharge regimes and, as well as plasma parameters, depends strongly on magnetic configuration. LF spectra are shown in Fig.8 for various values of I_{up}. At small I_{up}=23 mA, oscillations has narrow spectrum with maximum around 650 kHz and are localized at the periphery of the discharge column (Fig.9), where the density gradient is quite strong. Around location of the LF noise the dc radial electric field, as well as the rf field [11], is small. Thus, these oscillations are, most probably, driven by the azimuthal diamagnetic electron drift current. Measurements with the double probe show that oscillations are well correlated and propagate azimuthally with the IA velocity.

With increasing I_{up}, the discharge intensity grows and LF noise spreads over the whole cross-section. Its spectrum becomes continuous and broad (Fig.8) and the amplitude grows considerably (Fig.9). Correlation of oscillations falls sharply, so that wave propagation direction becomes uncertain. At higher I_{up}, noise has a wide spectrum with maximum around 0.7 MHz and is distributed radially with maximum in the range where the density gradient is weak but a strong radial field exists (Fig.9). Therefore, a probable reason for excitation of these oscillations is the azimuthal electric drift of electrons. Parametric instability can also arise, since a strong rf field exists in this region [11].

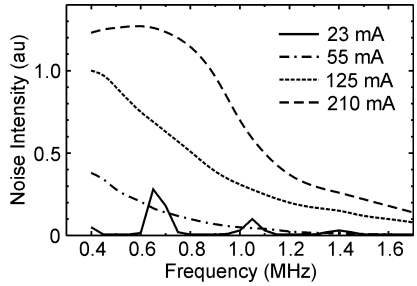

Fig.8. Envelopes of LF spectra, at r *= 6 cm and* z*= 25 cm*

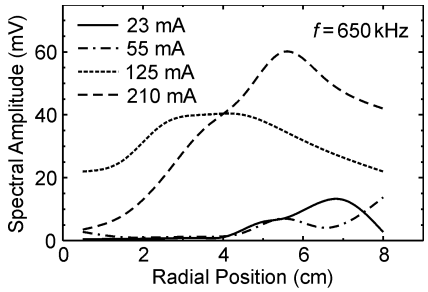

Fig.9. Radial profiles of the amplitude of LF oscillations

4. DRIVING MECHANISMS OF THE IA ACTIVITY

As long as the waves from continuous component of the LF spectra were argued to result from the electron drift current, we analyzed the appropriate instability for conditions of our experiments. Continuous spectra have maxima in the frequency range 0.2…0.5 MHz, which relates to quite short waves of lengths <1.5 cm, much shorter than the discharge chamber size. For this reason, we considered the model with planar geometry [12] and modified it to account properly for the particle collisions. We assumed electrons to flow across the magnetic field with velocity u and considered the following standard parameters relating to the experiments: B_0=

70 G, n_0 =4×10^{11} cm^{-3}, p_{Ar} =5 mTorr, T_e =4 eV, and T_i = 0.2 eV.

Dispersion of unstable waves computed for the standard parameters is shown in Fig.10. The growth rate first increases with the wave number, comes to maximum at $k\rho_e \approx 0.5$ (ρ_e is the electron Larmour radius), and then gradually falls. The growth rate becomes negative at $k\rho_e \approx 14$ (not shown in Fig.10) due to stabilizing effect of the ion Landau damping. The frequency exceeds the ion-acoustic frequency, at lower k, and approaches to $\omega_S = kv_S(1 + 3T_i/T_e)^{1/2}$, at higher k.

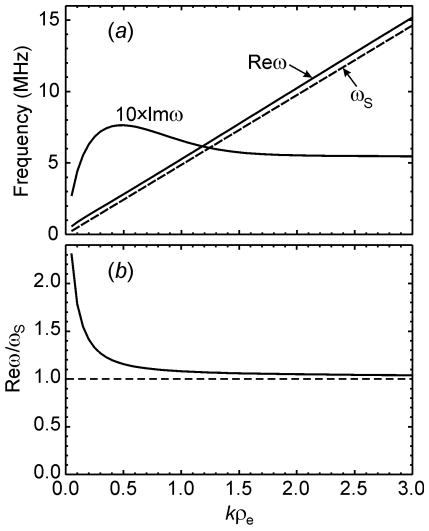

Fig.10. Frequencies and growth rates of unstable waves, at standard conditions, u/v_S =5, and $\cos\theta$ =3μ [θ is the wave propagation angle and $\mu = (m_e/m_i)^{1/2}$]

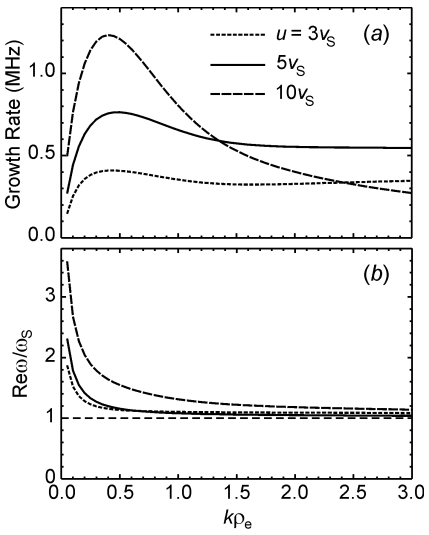

Fig.11. Dispersion of unstable waves, at various electron drift velocities. Standard parameters and $\cos\theta = 3\mu$

The effect of frequency enhancement at lower k is found to arise from electron collisions. Indeed, consider the longitudinal drag on electrons

$$F_{ez} = [e\partial\phi/\partial z - (T_e/n)\partial n/\partial z] - \nu_e m_e u_z, \qquad (1)$$

where ν_e and u_z are, respectively, the electron collision frequency and velocity perturbation. At low collisions, $\omega \nu_e << k_z^2 v_{te}^2$ where k_z is the longitudinal wave number and v_{te} the electron thermal velocity, the first two terms in the RHS of Eq.(1) are dominant and the routine Boltzman regime arises. If the collisions are high enough, so that $\omega \nu_e >> k_z^2 v_{te}^2$, the last term in the RHS of Eq.(1) exceeds the pressure term and electrons get into the dissipative regime, which gives rise to frequency enhancement. Just the latter regime is valid for the waves with lower k (Fig.10,b).

Dependence of the dispersion of unstable oscillations on the electron drift velocity is shown in Fig.11. With increasing u, the growth rate rises, especially in the range of maximum, and the wave frequency also

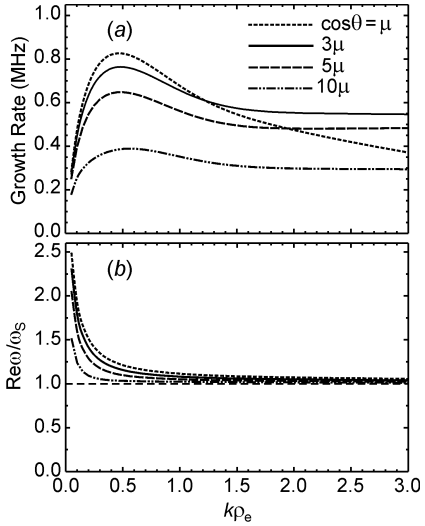

Fig.12. Dispersion of unstable waves, at various propagation angles. Standard parameters and $u/v_S = 5$

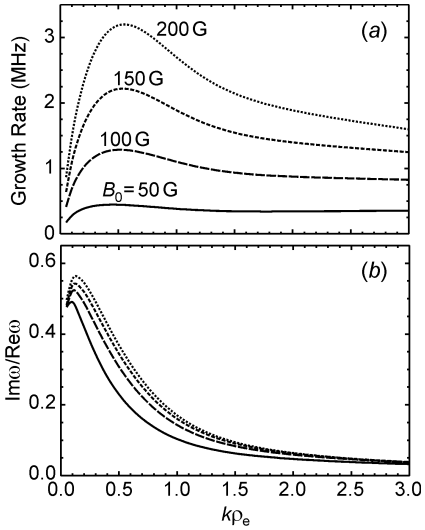

Fig.13. Dispersion of unstable waves, at various magnetic fields. Standard parameters, $u/v_S = 5$, and $\cos\theta$=3 μ

rises in the range of lower k. The growth rate and frequency grow with increasing the angle of the wave propagation relative to the magnetic field, as seen from Fig.12.

The effect of magnetic field on the wave dispersion is demonstrated in Fig.13. As seen, the growth rate rises

with the field, and location of the growth rate maximum moves towards shorter wavelengths, approximately as $\lambda_{max} \approx 4\pi\rho_e$ [Fig.13,a]. The growth rate is found to be less than the frequency at any magnetic fields and wave numbers [Fig.13,b]; i.e., the instability is weak. The maximum value of the growth rate is quite small at lower magnetic fields, B_0<50 G, and grows linearly with B_0 at higher fields.

We have also analyzed the structure of the global IA modes in a cylindrical geometry, for plasma column confined radially by an insulating wall while axially by the conducting flanges. All perturbations relating to the modes were supposed to have the form ~f(r)exp[i(k_zz+m θ−ωt)]. Fig.14 shows the radial profiles of the amplitude of electric potential of the modes with high azimuthal numbers m.

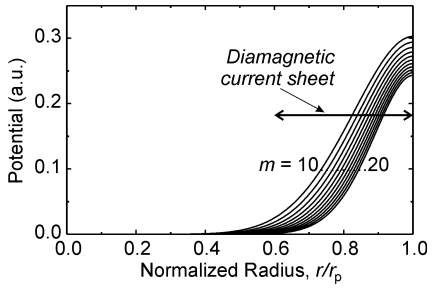

Fig.14. Radial profiles of the potential, for various global IA modes with high azimuthal numbers

Computations were conducted for the density and temperature profiles taken from the experiment on the helicon source (Fig.14). The modes are localized at the periphery of the plasma column, just within a sheet of the diamagnetic drift current that was detected in the experiment. Dispersion of various azimuthal modes computed for the basic axial mode, $k_z = \pi/L$ (L is the plasma length), with the effect of electron drift current neglected, is shown in Fig.15. The frequencies of computed modes are found to be separated by 9 kHz, which is quite close to experimentally measured value of 12.5 kHz (Sec.2). With increasing m, the damping rate grows rapidly; this is a result of that with increasing frequency the electrons get into the dissipative regime discussed earlier.

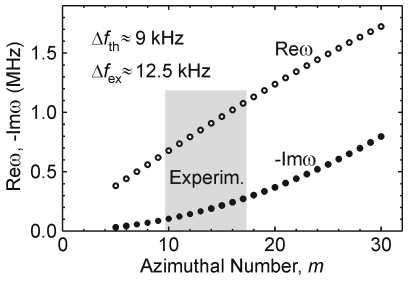

Fig.15. Frequencies and damping rates of various azimuthal IA eigenmodes

Ion-acoustic waves can also arise from the parametric instability driven due to rf oscillations of electrons relative to practically immobile ions. In helicon plasmas, the total driving electric field is a combination of the fields of the helicon wave and of the electrostatic wave excited due to linear mode conversion. Figure 16 shows the amplitude of the electron oscillatory velocity across the magnetic field, v_E, which was computed for the helicon source at standard parameters.

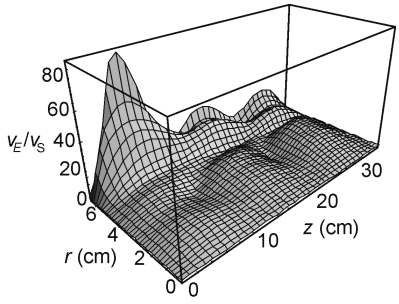

Fig.16. The amplitude of the electron oscillatory velocity in the helicon plasma, at antenna current of 5 A

As seen, v_E has maximum under the antenna and falls away from the antenna. However, even quite far from the antenna, at z =18 cm (where experimental measurements were done), v_E considerably exceeds the IA velocity v_S. As long as the characteristic scale of nonuniformity of electron oscillations is much larger than the IA wavelengths, we assumed the rf pump in the dipole approximation, i.e., as uniform, and used the model [13,14] that was modified to include properly the particle collisions.

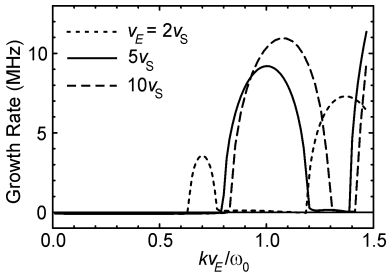

Fig.17. The growth rate of the parametric instability, at various values of the electron oscillatory velocity

The growth rates of the LF oscillations computed as functions of the wave number are shown in Fig.17, for various values of the oscillatory velocity. One can see two unstable bands with growth rates exceeding considerably the growth rates of the electron drift current driven instability (cf. Figs.11-13). The instability arises when $v_E > v_S$, and the maximum growth rates and the widths of unstable bands grow with increasing v_E. Frequencies of oscillations were found to grow with v_E and to exceed considerably the IA frequency; this effect is known to arise from strong coupling of oscillations to the rf pump [13].

CONCLUSIONS

Both the helicon plasma and the inductively coupled magnetized plasma operated at relatively low magnetic fields and input powers demonstrate the LF wave activity whose characteristics are affected strongly by the magnetic configuration. Depending on the regime, the wave spectra can include a broadband noise component

and/or spiky component. The LF oscillations were identified with the IA waves that propagate either azimuthally and radially, in case of the noise component, or only azimuthally, in case of the spiky component. The latter waves were measured to be the global azimuthal IA modes. Waves from the continuous spectrum were argued to arise due to the electron drift current while those from the spiky spectrum due to the parametric decay instability.

Theoretical analysis has shown that stationary electron drift currents can drive efficiently the IA waves, with growth rates exceeding the inverse lifetime of ions. Frequencies of shorter unstable waves are close to the IA frequency while frequencies of longer waves are higher due to onset of the dissipative regime for electrons. Parametric instability has much higher growth rates, but applies to quite short waves only. Note that this instability has to raise strongly the wave frequencies, as compared with the IA frequency, but this effect was not observed experimentally.

ACKNOWLEDGMENTS

This work was supported by the Science and Technology Center in Ukraine under contract №3068.

REFERENCES

1. A.I. Akhiezer, V.S. Mikhailenko and K.N. Stepanov. Ion-sound parametric turbulence and anomalous electron heating with application to helicon plasma sources // *Phys. Lett*. 1998, v.A245, №2, p.117-122.
2. V.S. Mikhailenko, K.N. Stepanov and E.E. Scime. Strong ion-sound parametric turbulence and anomalous anisotropic plasma heating in helicon plasmas // *Phys. Plasmas*. 2003, v.10, №6, p.2247-2253.
3. N.M. Kaganskaya, M. Krämer and V.L. Selenin. Enhanced-scattering experiments on a helicon discharge // *Phys. Plasmas*. 2001, v.8, №10, p.4694-4697.
4. J.L. Kline, E.E. Scime, R.F. Boivin, A.M. Keesee, X. Sun and V.S. Mikhailenko. Rf absorption and ion heating in helicon sources // *Phys. Rev. Lett*. 2002, v.88, №19, 195002.
5. V.F. Virko, G.S. Kirichenko and K.P. Shamrai. Parametric ion-acoustic turbulence in a helicon discharge // *Plasma Sources Sci. Technol*. 2003, v.12, №2, p.217-224.
6. C.S. Corr, N. Plihon, P. Chabert, O. Sutherland and R.W. Boswell. Spatially limited ion acoustic wave activity in low-pressure helicon discharges // *Phys. Plasmas*. 2004, v.11, №10, p.4596-4602.
7. B. Lorenz, M. Krämer, V.L. Selenin and Yu.M. Aliev. Excitation of short-scale fluctuations by parametric decay of helicon waves into ion–sound and Trivelpiece–Gould waves // *Plasma Sources Sci. Technol*. 2005, v.14, №3, p.623-635.
8. V.F. Virko, K.P. Shamrai, G.S. Kirichenko and Yu.V. Virko. Wave phenomena, hot electrons and enhanced plasma production in a helicon discharge in a converging magnetic field // *Phys. Plasmas*. 2004, v.11, №8, p.3888-3897.
9. R.L. Stenzel. Lower-hybrid turbulence in a nonuniform magnetoplasma // *Phys. Fluids*. 1991, v.B3, №9, p.2568-2581.
10. V.M. Slobodyan, V.F. Virko, G.S. Kirichenko and K.P. Shamrai. Helicon discharge excited by a flat antenna along a magnetic field // *VANT*. 2003, №4, p.235-240 (in Russian).
11. K.P. Shamrai, S. Shinohara, V.F. Virko, V.M. Slobodyan, Yu.V. Virko and G.S. Kirichenko. Wave stimulated phenomena in inductively coupled magnetized plasmas // *Plasma Phys. Control. Fusion*. 2005, v.47, №5A, p.A307-315.
12. C.N. Lashmore-Davies and T.J. Martin. Electrostatic instabilities driven by an electric current perpendicular to a magnetic field // *Nuclear Fusion*. 1973, v.13, №2, p.193-203.
13. Yu.M. Aliev, V.P. Silin and C. Watson. Parametric resonance in a plasma immersed in a magnetic field // *Zh. Eksp. Teor. Fiz*. 1966, v.50, №4, p.943-953. [*Sov. Phys. JETP*. 1966, v.23, p.626].
14. M. Porkolab. Parametric processes in magnetically confined CTR plasmas // *Nucl. Fusion*. 1978, v.18, №3, p.367-413.

ИОННО-АКУСТИЧЕСКАЯ ВОЛНОВАЯ АКТИВНОСТЬ В $m = 0$ ГЕЛИКОННОЙ ПЛАЗМЕ

К.П. Шамрай, В.Ф. Вирко, В.М. Слободян, Ю.В. Вирко, Г.С. Кириченко

Представлены результаты экспериментальных и теоретических исследований низкочастотной (НЧ) волновой активности в геликонной плазме и в индуктивно связанной замагниченной плазме. Эта активность показана относительно ионно-звуковых (ИЗ) волн, спектр которых может быть как шумовой и непрерывный, так и спайки или комбинированный. Природа активности устанавливалась из корреляционных измерений волновых характеристик, стационарных плазменных параметров и плазменного диамагнитного отклика. Обсуждаются различные механизмы возникновения ИЗ волн.

ІОННО-АКУСТИЧНА ХВИЛЕВА АКТИВНІСТЬ У $m = 0$ ГЕЛІКОННІЙ ПЛАЗМІ

К.П. Шамрай, В.Ф. Вірко, В.М. Слободян, Ю.В. Вірко, Г.С. Кириченко

Представлені результати експериментальних та теоретичних досліджень низькочастотної (НЧ) хвильової активності у геліконній плазмі та в індуктивно зв'язаній замагніченій плазмі. Ця активність показана відносно іонно-звукових (ІЗ) хвиль, спектр котрих може бути як шумовим і неперервним, так і спайки або комбінований. Природа активності встановлювалась із кореляційних вимірювань хвилевих характеристик,

стаціонарних плазмових параметрів та плазмового діамагнітного відгуку. Обговорюються різні механізми виникнення ІЗ хвиль.